Cabut, a C_2H_2 zinc finger transcription factor, is required during *Drosophila* dorsal closure downstream of JNK signaling

Silvia Muñoz-Descalzo, Javier Terol[1] and Nuria Paricio[2]

Departamento de Genética, Facultad CC Biológicas, University of Valencia, Dr. Moliner 50, 46100 Burjasot, Spain

[1]Present address: Javier Terol Alcayde
Centro de Genómica
Instituto Valenciano de Investigaciones Agrarias (IVIA)
Carretera Moncada - Náquera, Km. 4,5
46113 Moncada (Valencia)

[2]Corresponding author:
Phone 34-96 354 3005
Fax 34-96 354 3029
e-mail: "nuria.paricio@uv.es"

ABSTRACT

During dorsal closure the lateral epithelia on each side of the embryo migrate dorsally over the amnioserosa and fuse at the dorsal midline. Detailed genetic studies have revealed that many molecules are involved in this epithelial sheet movement, either with a signaling function or as structural or motor components of the process. Here we report the characterization of *cabut* (*cbt*), a new *Drosophila* gene involved in dorsal closure. *cbt* is expressed in the yolk sac nuclei and in the lateral epidermis. The Cbt protein contains three C_2H_2-type zinc fingers and a serine-rich domain, suggesting that it functions as a transcription factor. *cbt* mutants die as embryos with dorsal closure defects. Such embryos show defects in the elongation of the dorsal-most epidermal cells as well as in the actomyosin cable assembly at the leading edge. A combination of molecular and genetic analyses demonstrates that *cbt* expression is dependent on the JNK cascade during dorsal closure, and it functions downstream of Jun regulating *dpp* expression in the leading edge cells.

Keywords: *Drosophila*; Cabut; morphogenesis; dorsal closure; zinc finger; JNK; yolk cell nuclei

Running Title: Role of *cabut* in dorsal closure

INTRODUCTION

During *Drosophila* embryogenesis, dorsal closure, germband retraction, and head involution compose the major morphogenetic movements that participate in organogenesis of the first instar larva. Dorsal closure (DC) is the last of these movements that occurs following germband retraction. At the onset of closure, the epidermis of the *Drosophila* embryo has a hole on its dorsal side that is occupied by the amnioserosa, an epithelium of large flat cells that do not contribute to the larva. During DC, the lateral epithelia on each side of the embryo migrate dorsally over the amnioserosa and fuse at the dorsal midline. This process involves dramatic and coordinated morphological changes of both the epidermal and amnioserosal cells (Jacinto et al., 2002). Recent studies have demonstrated that an extraembryonic tissue, the yolk sac, also contributes to DC (Narasimha and Brown, 2004;Reed et al., 2004).

The movement of the epidermal sheets is directed by the dorsal most row of epidermal cells, which are in contact with the amnioserosa (Noselli and Agnes, 1999). At the beginning of DC, these dorsal-most epithelial (DME) cells elongate along the dorsoventral (D-V) axis of the embryo. This seems to be achieved by the accumulation of large quantities of filamentous actin (F-actin) and non muscle myosin at their interface with the amnioserosa, which is known as the leading edge (Young et al., 1993). First, the accumulation of actin occurs between cells at the level of adherens junctions, but later on, a cable of actin and myosin assembles across the leading edge (LE), and F-actin is incorporated into dynamic protrusions (Kaltschmidt et al., 2002). It seems that actin dynamics at the LE is preceded by the planar polarization of the DME cells associated with a reorganization of the cytoskeleton. This is reflected by the redistribution of several cell-surface-associated proteins in the plane of the epithelium that occurs towards the end of DC. For example, the distribution of the septate-junction-associated proteins Disc large (Dlg) and Fasciclin III (FasIII) changes as DC occurs.

At the beginning of DC they are distributed symmetrically around the epidermal cells, but as closure progresses they clear from the apical membrane facing the LE. The planar polarization of these cells is essential for DC since in its absence the process occurs abnormally (Kaltschmidt et al., 2002).

During DC cell shape changes in the amnioserosa begin with apical constriction of cells at the anterior and posterior ends of the tissue. The middle cells in between the two clusters also change shape since they are first elongated perpendicular to the A-P axis of the embryo, but at the end of DC they are both elongated along the A-P axis and apically constricted (Harden et al., 2002). This cell shape change is accompanied by an invagination of the tissue. Laser ablation experiments show that the amnioserosa is not passively squeezed by the advancing epithelial sheets, but exerts some tension that helps to draw them together (Kiehart et al., 2000). Recently, it has been shown that the basal surface of the amnioserosa is in close apposition with the yolk sac membrane. This intimate contact between these two extraembryonic tissues is mediated by integrins and prevents premature anoikis of the amnioserosa, suggesting that the yolk cell contributes to dorsal closure since it is essential for amnioserosa survival (Narasimha and Brown, 2004; Reed et al., 2004).

Genetic analyses have identified numerous genes required for DC. DC mutants die during embryogenesis and present various shapes and sizes of holes in cuticle preparations of the resulting larvae (Jacinto and Martin, 2001). Molecular analyses of these genes have revealed that some of them encode gene products that are structural and motor components of the process. That is the case of *zipper* (*zip*) or *canoe* (*cno*), which code for the motor protein non-muscle myosin II and an adherens-junction-associated protein, respectively (Miyamoto et al., 1995; Young et al., 1993). Besides, several signaling pathways like the Jun N-terminal kinase (JNK) cascade and Wg signaling are also important in regulating the initiation and maintenance of epithelial movements associated with DC (reviewed by Harden, 2002). Prior

to DC the JNK signaling cascade is active in both the amnioserosa and the LE of the epidermis (Reed et al., 2001). Later on, it is downregulated in the amnioserosa but not in the LE cells, activating the localized transcription of two target genes: *dpp* and a dual specifity phosphatase, *puckered* (*puc*) (Glise and Noselli, 1997; Martín-Blanco et al., 1998; Riesgo-Escovar and Hafen, 1997; Zeitlinger et al., 1997). It has been recently proposed that a subsequent activation of JNK signaling in the amnioserosa could trigger the disintegration and death of this tissue after closure of the epidermis (Reed et al., 2004). Besides, several studies of DC in embryos with impaired JNK and Wg signaling have also shown that both are essential for actin dynamics and cytoskeletal organization of the DME cells, but only Wg signaling seems to be required for the polarization of epidermal cells in the initial phases of DC (Kaltschmidt et al., 2002; McEwen et al., 2000; Morel and Martinez-Arias, 2004; Ricos et al., 1999).

In this paper, we report the identification and genetic analysis of *cabut* (*cbt*), a novel gene implicated in *Drosophila* embryogenesis. It is expressed in the yolk cell and in the lateral epidermis, and encodes a putative transcription factor containing C_2H_2 zinc finger motifs. Phenotypic analyses of *cbt* mutant embryos show that loss of Cbt function affects several key events in DC: cell shape change in the epidermis, cytoskeleton activity, JNK signaling, and occasionally polarity of the DME cells**.** Taken together, our results indicate that *cbt* has a role in DC, downstream of the JNK cascade, regulating *dpp* expression at the LE.

MATERIALS AND METHODS

Fly strains

The EP line *EP(2)2237* (Rørth et al., 1998) was used for the characterization of the *cbt* locus. We mobilized the EP element in that line using the Sp/CyO; Sb, Δ2-3/TM6, Ubx stock as external source of transposase and several imprecise lethal excisions were recovered. The Tp(2;1)$odd^{1.10}$ transposition line (Nusslein-Volhard et al., 1985) was used to confirm the genomic location of the excision alleles.

The UAS-*cbt* wild type construct was obtained by cloning the SD06353 cDNA into the pUAST *Drosophila* transformation vector (Brand and Perrimon, 1993). P-element-mediated *Drosophila* germ-line transformation of this construct was performed as described (Spradling and Rubin, 1982).

The following GAL4 and UAS lines were also used: *69B*-GAL4, *da*-GAL4 (both from Bloomington), *en*-GAL4 (Tabata et al., 1995), *arm*-GAL4 (Sanson et al., 1996), *P0180*-GAL4 (Narashima et al., 2004), UAS-Hep^{ACT} (Weber et al., 2000), UAS-*dpp* (a gift from S. Casas). The mutant alleles used in this work are: bsk^{2} (Sluss et al., 1996), jun^{2} (Nusslein-Volhard et al., 1984), mys^{1} (Digan et al., 1986), puc^{E69} (Ring and Martinez-Arias, 1993) and $bsg^{B39.1M2}$ (Reed et al., 2004).

To distinguish the $cbt^{EP(2)2237E1}$ and $cbt^{EP(2)2237E28}$ homozygous mutant embryos from their heterozygous siblings, we made use of balancer chromosomes carrying a *lacZ* (CyO,*wg-lacZ*; Ingham et al., 1991) or a *GFP* (CyO,*ubi-GFP*; Bloomington) transgene.

Molecular analyses

The exact point of the EP element insertion in the *EP(2)2237* line was determined by inverse PCR as described in the BDGP web site. PCR products were cloned in TOPO 2.1 (Invitrogen) and sequenced. Searches in *Drosophila* databases using those sequences identified several

ESTs within the immediate vicinity of the EP insertion. Two of them were selected for sequence analysis: LD06353 and SD05727. We fully sequenced LD06353 (GenBank accession no. **AJ749862**), which corresponds to the *cbt-RA* isoform. Partial sequencing of SD05727 revealed that it is identical in sequence to SD05726 (data not shown) and corresponds to the *cbt-RB* isoform. To determine the exon-intron structure of *cbt*, we compared the genomic and the ESTs sequences from BDGP, and also the cDNA sequences determined by us. We found 23 ESTs derived from the *cbt* gene: 20 correspond to the *cbt-RA* isoform, two correspond to the *cbt-RB* isoform, and one is a partial sequence that could correspond to either of them.

To determine the molecular lesion present in the mutants, we performed single-embryo DNA amplifications of non-GFP embryos collected from $cbt^{EP(2)2237E1}$/CyO,*ubi-GFP* and $cbt^{EP(2)2237E28}$/CyO, *ubi-GFP* stocks using different pairs of primers to amplify overlapping fragments encompassing the whole *cbt* coding region. These PCR products were purified and cloned in TOPO 2.1 for sequencing. In the $cbt^{EP(2)2237E28}$ allele, we found 30 additional bp at the EP-element insertion point (19 bp correspond to the EP-element, and 11 bp are a genomic duplication). The coding region of $cbt^{EP(2)2237E1}$ allele was wild type. A set of primers were designed to amplify the genomic region 0.5 kb downstream (including the 3´UTR from *Arc105*) and 4.9 kb upstream of the *cbt* locus (see Supplementary material). Primers between 3.9 kb and 4.9 kb upstream of *cbt* (5´-AGACGACCTTCAGTCGGG-3´ and 5´-GCTGTTCACGTTGACTTC-3´) failed to amplify the expected product in $cbt^{EP(2)2237E1}$ homozygous embryos as they did in wild-type, in *EP(2)2237* and in $cbt^{EP(2)2237E28}$ homozygous embryos.

In situ hybridization

In situ hybridizations to whole-mount embryos were performed as described (Tautz and Pfeifle, 1989). In situ hybridizations to imaginal discs were done following the protocol described by Cheung et al. (1992) with several modifications. Antisense RNA probes were generated with the DIG RNA labeling kit SP6/T7 (Roche). The wild-type *cbt* expression pattern was determined in *OrR* embryos using the SD06353 cDNA as template for riboprobe synthesis. A complete *dpp* cDNA (Lockwood and Bodmer, 2002) was used to generate *dpp* antisense riboprobes. Sense probes generated in parallel with the same templates were used as negative controls in all cases.

RT-PCR and Northern blot

Total RNA was isolated from 0-22h embryos using Tri-Reagent (Sigma) following the supplier´s instructions. RT-PCRs were performed with RNA from w^- embryos. The reverse primer used to detect both *cbt* isoforms was 5´-CCTCGGACATTGTTGGCG-3´; the forward primer for the *cbt-RB* isoform was 5´-TGGGTCAATGCTGGTCAG-3´ and for the *cbt-RA* isoform was 5´-GGATACCTTGCTACCTTC-3´. For the Northern blot, total RNA (30 µg per lane) from w^-, $cbt^{EP(2)2237E1}$ and $cbt^{EP(2)2237E28}$ homozygous embryos and *arm*-GAL4/UAS-*cbt* embryos was separated by formaldehyde gel electroforesis and blotted onto a positively charged nylon membrane (Roche). *cbt* and *RP49* antisense RNA probes were generated as described. Hybridization and washes were performed as described by the supplier (Roche). The blots were detected immunochemically with CDP-Star (Roche).

Embryo phenotypic analysis

Embryos for SEM were prepared as described (Jacinto et al., 2002), except that the vitelline membrane was removed using heptane-methanol 1:1. Specimens were imaged on a Hitachi S-2500 scanning electron microscope. For cuticle analysis, embryos were collected during 24 h

and aged an additional 24 h, then they were dechorionated in commercial bleach for 3 minutes, and the vitelline membrane removed using heptane-methanol 1:1. After several washes in methanol, embryos were mounted in Hoyer´s-lactic acid 1:1 and allowed to clear at 65ºC overnight. Some homozygous mutant embryos showed a bigger head than wild types. This led us to name this gene *cabut*, which means "bigheaded" in the dialect of Valencia. These "bigheaded" embryos have a very weak dorsal-open phenotype.

Embryonic lethality assays

The embryonic lethality rescue of the $cbt^{EP(2)2237E1}$ homozygous mutant overexpressing UAS-*cbt* was performed using several GAL4 lines (*X*-GAL4, were *X* can be *69B*, *da* or *P0180*; all on the third chromosome and homozygous viable). For these assays we performed the following crosses: $cbt^{EP(2)2237E1}$/CyO with *X*-GAL4 homozygous flies and $cbt^{EP(2)2237E1}$/CyO with UAS-*cbt*/TM3 flies. The non-balanced offspring of both crosses was then crossed together, and we measured the percent embryonic lethality in this cross. If there was no rescue, we would expect 25% embryonic lethality: 18.25% corresponding to $cbt^{EP(2)2237E1}/cbt^{EP(2)2237E1}$;Y/+ (were Y can be UAS-*cbt*, *X*-GAL4 or the wild-type chromosome) embryos and 6.25% corresponding to $cbt^{EP(2)2237E1}/cbt^{EP(2)2237E1}$;*X*-GAL4/UAS-*cbt* embryos. If there is any rescue, the embryonic lethality will be reduced. As all the embryos homozygous mutant for $cbt^{EP(2)2237E1}$ die, we can calculate the absolute embryonic lethality rescue as: (25%-observed % embryonic lethality)/6.25% x 100 (Table 1). The embryonic lethality rescue of the $cbt^{EP(2)2237E1}$ homozygous mutant overexpressing UAS-*dpp* was performed similarly, but using only the *69B*-GAL4.

To test for genetic interactions between *cbt* and *hep*, we performed the following cross: $cbt^{EP(2)2237E1}$/CyO with *69B*-GAL4 homozygous flies. The non-balanced offspring was then crossed to UAS-Hep^{Act} homozygous flies, and we measured the percent embryonic lethality

in such cross. If there was not genetic interaction, we would expect 50% embryonic lethality: 25% corresponding to *69B*-GAL4/UAS-Hep^{Act} embryos and 25% corresponding to embryos that overexpress Hep^{Act} and contain the $cbt^{EP(2)2237El}$ allele. If *cbt* is downstream of *hep*, the embryonic lethality will be reduced. As all the embryos that overexpress Hep^{Act} die, we can calculate the embryonic lethality due to the genetic interaction as: 100-[(50%-observed % embryonic lethality)/25% x 100] (Table 2).

Histology and immunohistochemistry

Embryos were fixed and stained using standard protocols. Fixation was carried out using 4% parafolmaldehyde diluted in PBS and desvitellinization in heptane-methanol 1:1. We used the following primary antibodies: rabbit anti-Cno (1/200; Takahashi et al., 1998); rabbit anti-Dlg (1/200; Woods et al., 1996); mouse anti-FasIII (1/50; Developmental Studies Hybridoma Bank) and rabbit anti-myosin II heavy chain (1/1000; Jordan and Karess, 1997). The fluorescent-conjugated secondary antibodies (Calbiochem) were used at a 1/40 dilution. Specimens were mounted in Mowiol and examined under a Leica TCS SP2 confocal microscope. Several Z sections of each embryo were taken and processed. β-galactosidase was detected with a mouse antibody (1/200, Promega). For anti- β-galactosidase stainings, biotinylated secondary antibodies were used in combination with the Vectastain Elite ABC kit. Anti-β-galactosidase and in situ hydridization double stainings were done as described (Manoukian and Kraus, 1992).

RESULTS

Molecular characterization of *cabut*

cabut (*cbt*) was identified in a modular misexpression screen of 2200 different EP lines (Rørth et al., 1998) looking for genes involved in the establishment of epithelial planar cell polarity, as an insertion (*EP(2)2237*) that caused planar polarity defects in the eye, wing and thorax when expressed under the control of *sev*-GAL4 and *ap*-GAL4, respectively (Marek Mlodzik and N.P., unpublished). To identify the gene overexpressed by *EP(2)2237*, we cloned and sequenced the adjacent DNA and identified corresponding ESTs in the BDGP database. *EP(2)2237* is inserted 14 bp upstream of the predicted gene CG4427 in the Gadfly database (Fig. 1A). We have named this gene *cabut* (see Materials and methods), which is located at position 21C6 on chromosome arm 2L. Two different mRNA products have been associated to *CG4427*, *CG4427-RA* and *CG4427-RB,* although our results indicate that *CG4427-RB* is probably an artifact (see below). *CG4427-RA* (hereafter called *cbt-RA*) mRNA encodes a protein of 428 amino acids that contains a serine-rich region at the amino terminus, and three classical zinc finger domains C_2H_2 type at the carboxy-terminal region (Fig. 1C), which are located in tandem and match the consensus sequence described as $CX_{2-4}CX_{12}HX_{2-6}H$ (Iuchi, 2001). An alignment of the three Zn fingers found in the Cbt protein is shown in Fig. 1D. Database searches identified many proteins with similar domains and from many different organisms (data not shown), most of them classified as Sp1-like transcription factors, Krüppel-like factors, TGFβ inducible early growth response proteins or BTE-binding proteins. In general, proteins with three C_2H_2 zinc fingers may bind DNA, RNA or proteins through the fingers, although most of them are DNA-binding proteins that, together with other factors, participate in controlling transcription of target genes (Iuchi, 2001). Thus, the probable role of Cbt is to bind to specific regions of DNA and to regulate gene expression.

Expression of *cbt* in embryos and imaginal discs

The spatial expression pattern of *cbt* in embryos and imaginal discs was examined by whole-mount in situ hybridization with a *cbt-RA* RNA probe. The initial expression of *cbt* is observed at the cellular blastoderm stage in an ubiquitous manner (Fig. 2A). This ubiquitous expression persists till stage 8. Then, at stage 9 *cabut* is mainly expressed in the gut primordium and also in the epidermis (data not shown). During stage 11 and onwards, *cabut* is expressed in the yolk cell nuclei and in the lateral epidermis (Figs. 2B-C). *cbt* expression in the yolk cell has been confirmed by using an enhancer trap line in the *basigin* (*bsg*) gene (Fig. 2C), which is expressed in that tissue (Reed et al., 2004). Moreover, *cbt* transcripts can also be detected in the posterior gut (Fig. 2B). At later stages, when the yolk cell is included in the gut, expression of *cbt* is also present there. In third instar larvae, *cbt* expression is largely ubiquitous in all imaginal discs (data not shown). Similar hybridization experiments performed with RNA probes specific for the *cbt-RB* isoform yielded negative results. To confirm this, we performed RT-PCR experiments designed to distinguish between *cbt-RA* and *cbt-RB* isoforms in different stages of development. We could only detect *cbt* products when using primers specific for the *cbt-RA* isoform (data not shown). This indicates that the *cbt-RB* variant (indeed represented by only two ESTs in the BDGP, see Material and methods) probably corresponds to an artifact generated during cDNA preparation.

Genetics of the *cbt* locus

To generate *cbt* mutations we took advantage of the *EP(2)2237* element inserted in the upstream region of *cbt*, which is homozygous viable. Several lethal excisions were obtained after mobilization of the EP element, and two of them ($cbt^{EP(2)2237E1}$ and $cbt^{EP(2)2237E28}$) were used for further analyses. In order to identify the molecular lesions causing the lethality of those excisions, we amplified and sequenced the coding region of *cbt* from embryos

homozygous for both alleles, finding in $cbt^{EP(2)2237E28}$ mutants 30 additional bp in the original insertion site of the *EP(2)2237* element (Fig. 1B, see Materials and methods). In $cbt^{EP(2)2237E1}$ embryos, the *cbt* coding region was wild-type. Further PCR analyses of genomic regions upstream and downstream of the *cbt* coding region allowed us to identify the molecular lesion in $cbt^{EP(2)2237E1}$ embryos, since we failed to amplify a genomic region between 3.9 and 4,9 kb upstream of the *cbt* transcription start site (Supplementary Fig. 1). To demonstrate whether these mutations were affecting *cbt* expression, we performed in situ hybridization experiments. *cbt* expression was almost lost in $cbt^{EP(2)2237E1}$ homozygous embryos, although it is weakly detected in the gut (Fig. 2D). In $cbt^{EP(2)2237E28}$ homozygous embryos *cbt* expression was present in the epidermis and gut, but not in the yolk cell (Fig. 2E). These results were confirmed by Northern blot analyses using *cbt* specific probes. While in $cbt^{EP(2)2237E1}$ embryos *cbt* transcripts are weakly detected, in $cbt^{EP(2)2237E28}$ embryos the level of expression of the gene is almost wild type (Fig, 2F). In control embryos we detect only a 2-kb transcript corresponding to the *cbt-RA* isoform, thus confirming the results obtained by RT-PCR (see above). Our results suggest that the $cbt^{EP(2)2237E1}$ mutation is probably affecting an enhancer element necessary for *cbt* expression, and can be considered a *cbt* loss-of-function allele. However, $cbt^{EP(2)2237E28}$ appears to be a very weak allele, in which *cbt* expression is only reduced.

We also wanted to confirm genetically that the *cbt* genomic region was affected in both excision lines. To do that we used the transposition line $Tp(2;1)odd^{1.10}$, in which the *cbt* genomic region is transposed to the X chromosome (Nusslein-Volhard et al., 1985). We found that males heterozygous for any of both *cbt* alleles, and carrying the deficiency but not the transposition, were lethal. All these results are consistent with the notion that the both mutations affect the *cbt* genomic region and disrupts *cbt* activity.

Loss of *cbt* function is associated with defects in dorsal closure during embryogenesis

Since *cbt* is mainly expressed at the embryonic stage, we analyzed the phenotype of *cbt* mutant embryos. First, we determined the timing and cause of lethality associated with the $cbt^{EP(2)2237E1}$ allele. Lethal phase analysis showed that 100% of homozygous $cbt^{EP(2)2237E1}$ animals die during embryogenesis, at late embryonic stage. Cuticle preparations of $cbt^{EP(2)2237E1}$ mutant embryos showed that 98.3 % of them displayed a failure of dorsal closure with characteristic dorsal holes in their cuticles. The size of the holes in such embryos is variable (Figs. 3B-C), but it covers most of the dorsal region of the cuticle in 91.7% of the mutant embryos. The same analyses performed with the $cbt^{EP(2)2237E28}$ allele indicated that only 78% homozygous $cbt^{EP(2)2237E28}$ animals die during embryogenesis, and only 2.9% of them show anterior holes in cuticle preparations (Fig. 3D). This weak phenotype is consistent with our previous results regarding *cbt* expression in such mutants. Therefore we used the $cbt^{EP(2)2237E1}$ allele for further analyses. To better identify the processes leading to the defects observed in $cbt^{EP(2)2237E1}$ mutant embryos, scanning electron microscopy (SEM) was used to visualize embryonic morphology. At early stages of development *cbt* mutant embryos appear normal (Figs. 3E-F), but at stage 14 some of them show an abnormal shape of the amnioserosa tissue, suggesting that lateral epidermis elongation does not occur properly in those embryos (see below, Fig. 3G). By the end of embryonic development we see embryos with dorsal holes (data not shown), and others in which internal organs are extruded (Fig. 3H), due to an improper closure of these embryos.

To demonstrate that the lethality observed in $cbt^{EP(2)2237E1}$ mutant embryos is caused by loss of *cbt* activity, we attempted to rescue it by overexpressing *cbt* with *da*-GAL4 (an ubiquitous driver). Confirming our assumption, we found that ubiquitous *cbt* overexpression results in a 50.2% of rescue (Table 1). Since *cbt* is expressed in the epidermis and the yolk cell during embryogenesis, we wanted to test its requirement in both tissues. Similar lethality

rescue experiments of *cbt*$^{EP(2)2237E1}$ mutant embryos were performed by overexpressing *cbt* either with *69B*-GAL4 (an epidermal driver) or with *P0180*-GAL4 (a driver specific for the yolk cell). Overexpression of *cbt* in the epidermis results in a 100% of rescue. However, the lethality is partially rescued when *cbt* is overexpressed in the yolk cell (see Table 2) suggesting that *cbt* activity is mainly required in the epidermis for proper embryonic development.

Loss of *cbt* function affects cell shape changes in the epidermis but not in the amnioserosa

During DC, cells in the epidermis and the amnioserosa undergo shape changes and movements. Moreover, the DME cells polarize in the plane of the epithelium. To determine whether a failure in these events could be the cause of closure defects observed in *cbt* mutants, we stained *cbt*$^{EP(2)2237E1}$ mutant embryos for markers that allowed us to analyze cell shape and polarity in the dorsal ectoderm. Dlg and FasIII inmunostainings of those embryos revealed that the elongation in the D-V axis of DME cells, and more lateral epidermal cells, initiates properly but fails shortly afterwards. In consequence, those cells do not elongate to the same extent as in wild-type embryos, and round up (Figs. 4A-D). Moreover, we see that occasionally the distribution of Dlg and FasIII in the DME cells is not polarized, since it does not disappear from the apical part of the cells. Thus elongation and, in some cases, planar polarization of the DME cells do not occur properly in *cbt* mutant embryos.

In order to check whether amnioserosa morphogenesis was impaired in *cbt* mutants, we stained *cbt*$^{EP(2)2237E1}$ mutant embryos with a anti-Canoe (Cno) antibody, which provides a clear view of the shape of amnioserosal cells. Cell shape changes in the amnioserosa begin with apical constriction of cells at the anterior and posterior ends of this tissue. The middle cells in between the two clusters are elongated perpendicular to the A-P axis, but at the end of

DC they are both elongated along the A-P axis and apically constricted (Harden et al., 2002). Examination of $cbt^{EP(2)2237E1}$ mutant embryos revealed that morphogenesis of the amnioserosa is not affected by loss of *cbt* function (Figs. 4E-F and data not shown). Only amnioserosa attachment defects are occasionally seen in the mutants (Fig. 4F).

Cytoskeleton activity at the leading edge is disturbed in *cbt* mutant embryos

Besides to the temporally ordered redistribution of several cell-surface-associated proteins in the plane of the epithelium, the actin cytoskeleton reorganizes in the DME cells during DC. This is reflected by the accumulation of large quantities of non-muscle myosin and filamentous actin at the LE, which occurs in large aggregates or puncta (Kaltschmidt et al., 2002; Ricos et al., 1999). To determine whether this process occurs normally in *cbt* mutants, we examined the levels of non-muscle myosin in $cbt^{EP(2)2237E1}$ mutant embryos and compared them to wild-type embryos. (Fig. 5). Our results indicate that the aggregates are missing in the mutants, which show a feeble and irregular accumulation of myosin at the LE. This suggests that *cbt* is required for the cytoskeletal organization of the DME cells during DC. Defects in the accumulation of myosin at the LE during cable assembly have also been observed in embryos homozygous for mutations in members of the JNK cascade and in mutants for Wg signaling (Kaltschmidt et al., 2002; Ricos et al., 1999).

***cbt* acts downstream of the JNK cascade**

Genetic analyses have demonstrated that the JNK signal transduction cascade has a very important role during DC, regulating its progression and expression of genes at the LE (reviewed by Harden, 2002). Our analysis of epidermal and cytoskeletal phenotypes of *cbt* mutant embryos suggested that this gene could be related to the JNK pathway during this process. This prompted us to determine the epistatic relationships between *cbt* and

hemipterous (*hep*), a JNK pathway component (Glise et al., 1995). Expression of a constitutively activated form of Hep (Hep^{ACT}) in the epidermis with the *69B*-GAL4 driver causes 100% of embryonic lethality (Table 2), due to the overactivation of the JNK pathway. We have found that a reduction of the *cbt* gene dosage in such embryos, using the $cbt^{EP(2)2237EI}$ mutant allele, led to a reduction of the embryonic lethality to 36.4%. The direction of the genetic interaction between *cbt* and *hep* supports a role for *cbt* in JNK signal transduction, downstream of *hep*. As further confirmation of these results, we asked whether *cbt* expression could be modified in embryos with different levels of JNK activity. First, we analyzed *cbt* expression in embryos mutant for *basket (bsk*) or *jun,* which encode the the Jun N-terninal kinase (Riesgo-Escovar et al., 1996; Sluss et al., 1996) and the transcription factor Djun (Hou et al., 1997; Kockel et al., 1997), respectively. In both mutants, *cbt* expression is absent in the epidermis and the yolk cell (Figs. 6B-C). Conversely, we found that *cbt* expression can be induced ectopically by overexpression of a constitutively activated form of Hep (Hep^{ACT}) with *en*-GAL4 (Fig. 6D). Thus, all these findings suggest that *cbt* functions downstream of JNK signaling.

As previously mentioned, our in situ experiments showed that *cbt* expression is not only lost in the epidermis but also in the yolk cell, in which the JNK cascade has not been reported to be active. It is assumed that prior to DC, JNK signaling is downregulated in the amnioserosa (Reed et al., 2001) but as DC approaches to completion, it is upregulated in that tissue (Reed et al., 2004). Besides, it has been recently published that there are physical interactions between the amnioserosa and the underlying yolk cell, which are mediated by integrins (Narasimha and Brown, 2004; Reed et al., 2004). These contacts are accomplished by cellular extensions that might facilitate a signaling function between both tissues (Reed et al., 2004). We therefore asked whether *cbt* expression could be affected by mutations in the *myospheroid* (*mys*) gene, which encodes the βPS integrin (MacKrell et al., 1988). Our results

show that *cbt* expression in the yolk cell nuclei is absent in mys^{1} mutants, in which apposition of amnioserosa and yolk cell membranes is compromised (Narasimha and Brown, 2004). Conversely, *cbt* expression in the epidermis is not affected (Fig. 6E-F). Taken together, these results suggest that *cbt* expression in the yolk nuclei depends on JNK signaling and requires the physical interaction between the yolk cell and the amnioserosa, supporting the hypothesis that a signaling function could exist between both tissues.

cbt regulates _dpp_ expression at the leading edge

Since our previous results indicate that *cbt* expression is regulated by the JNK cascade, we wanted to know whether mutations in this gene could affect the expression of the two targets of JNK signaling during DC, which are *dpp* and *puc*. To test this, we first monitored *dpp* expression in wild-type and *cbt* mutant embryos. The wild-type expression of *dpp* is dynamic through embryogenesis, but in late embryonic stages is evident in two thin stripes (Fig. 7A), a dorsal stripe located at the LE, and a ventral stripe (Glise and Noselli, 1997; Riesgo-Escovar and Hafen, 1997). We find that *dpp* expression is abolished in LE epidermal cells in *cbt* mutant embryos, although the stripe located more ventrally is not altered (Fig. 7B). Moreover, we tested *dpp* expression in *arm*-GAL4/UAS-*cbt* embryos finding that ectopic *cbt* activity leads to an expansion of the domain of *dpp* expression at the LE (Figs. 7C-D). Besides, we find that overexpression of *cbt* with an *en*-GAL4 driver also induces ectopic expression of *dpp* (Fig. 7E). As previously reported, we see in both experiments that only a subpopulation of cells is competent to express *dpp* (Morel and Martínez-Arias, 2004). These data demonstrate that *cbt* is a positive regulator of *dpp* expression at the LE in the dorsal epidermis. An additional evidence indicating that *dpp* is downstream of *cbt* is the finding that *dpp* overexpression with *69B*-GAL4 is able to partially rescue the embryonic lethality of the $cbt^{EP(2)2237El}$ allele (see Table 1). The second JNK target gene activated in LE cells is *puc*

(Glise et al., 1995; Riesgo-Escovar et al., 1996). The expression of *puc* was measured by using a *puc*-lacZ enhancer trap (Ring and Martínez-Arias, 1993). Our results indicate that *puc* expression is not altered in the mutants (Figs 7F-G), suggesting that *cbt* functions in the JNK pathway, and downstream of *jun*, to control *dpp* expression.

DISCUSSION

In this report we describe the characterization of *cabut*, a new *Drosophila* gene. It encodes a zinc finger-containing protein, and is expressed in the lateral epidermis and the yolk cell nuclei. Genetic and phenotypic analyses indicate that *cbt* is required for proper DC. We have shown that a reduction in Cbt function affects several key events during DC: shape changes of the DME cells, cytoskeleton dynamics and JNK signaling. Based on molecular data and genetic interactions, we show that Cbt acts downstream of the JNK cascade in the epidermis and regulates *dpp* expression in the LE cells. Our results also suggest the existence of a signaling function between the amnioserosa and the yolk cell, which would account for the JNK-dependent expression of *cbt* in the yolk cell nuclei.

Role of *cabut* in dorsal closure

Our phenotypic analysis of *cbt* mutants shows that this gene is required during *Drosophila* DC. Embryos homozygous for a *cbt* loss-of-function allele exhibit abnormal closure, reflected by the presence of dorsal-anterior holes. DC is a very complex morphogenetic movement that requires the combined effects of different tissues and involves activation of cytoskeletal machineries and signaling pathways (Harden, 2002). Thus, DC results from a sequence of coordinated events, and defects in any of them lead to a failure of the whole process. Our data indicate that *cbt* mutant embryos show several defects in the DME cells during DC that can be responsible of the closure phenotypes observed. First, the morphology of the DME cells is abnormal in the mutants, since they do not elongate properly. Second, mutations in *cbt* affect the cytoskeletal machinery in LE cells. During DC, LE cells assemble an actomyosin cable that is necessary to maintain a uniform epithelial advance (Martin and Wood, 2002). In *cbt* mutants we observe an aberrant cable assembly, which shows a very feeble accumulation of myosin. Third, the polarization of these cells, reflected by the redistribution of cell-surface-

associated proteins along the D-V plane (like FasIII or Dlg), is sometimes affected in *cbt* mutants. In those cases such proteins are not cleared from the dorsal most edge of the cells as occurs in wild type embryos at the onset of closure. By contrast, morphogenesis of the amnioserosa appear to occur normally in absence of *cbt* function. Thus, based on the phenotypes seen in *cbt* mutant embryos, we conclude that *cbt* is required at different steps in DC. In particular, it is necessary for elongation of the DME cells in the dorso-ventral axis and for the assembly of the actomyosin cable at the LE. Its involvement during polarization of the DME cells is not clear, since the phenotype observed in the mutants is not very strong. Similar DC phenotypes have been found in mutants lacking components of the JNK cascade (Harden, 2002; Kaltschmidt et al., 2002; Ricos et al., 1999), suggesting that *cbt* could be related to JNK signaling.

cbt functions downstream of the JNK cascade

Several lines of evidence have confirmed that *cbt* acts downstream of JNK signaling during DC. First, *cbt* loss of function is able to partially rescue the lethality caused by overexpression of an activated form of Hep in the epidermis. This result is in agreement with a role of *cbt* downstream of the JNK module. Second, analyses of *cbt* expression in embryos mutant for JNK cascade components, like *bsk* or *jun*, show that this expression is absent in the epidermis and the yolk sac, but not in the gut. This indicates that, at least in those tissues, *cbt* expression is dependent on JNK activation, and confirms our previous result. Besides, we were able to induce *cbt* expression in stripes by overexpressing an activated from of Hep with an *en*-GAL4 driver Third, analysis of the expression of *dpp* and *puc*, two target genes activated in response to JNK signaling in the LE cells during DC (Glise and Noselli, 1997; Martín-Blanco et al., 1998; Riesgo-Escovar and Hafen, 1997; Zeitlinger et al., 1997), in *cbt* mutant embryos reveals that *dpp* but not *puc* expression is lost in the mutants. Moreover, *dpp* expression can

be induced ectopically by overexpression of *cbt*. Taken together, our results indicate that *cbt* acts downstream of the JNK cascade and the AP-1 transcription factor Jun, regulating *dpp* expression at the LE. Regarding this, we have found putative AP-1 binding sites in the genomic region located upstream of the *cbt* transcription unit (data not shown). It is tempting to speculate that *cbt* expression is directly regulated by Jun through binding to that genomic region. Further experiments will be required to confirm this hypothesis.

Wg signaling is also required for DC. Indeed it regulates cytoskeleton activity at the LE and is also required for the polarization of the DME cells (Kaltschmidt et al., 2002; Morel and Martínez-Arias, 2004; Ricos et al., 1999). Since we found that polarization of the DME cells is not complete in some *cbt* mutant embryos, this raised the possibility that *cbt* might be related to Wg signaling. To test this, we analyzed *cbt* expression in *arm* and *dsh* mutants. Our results show that *cbt* expression is not affected in the mutants (data not shown), indicating that Wg signaling is not required for *cbt* expression. This will explain that defects during this polarization of the DME cells are only occasionally observed in *cbt* mutant embryos, and confirms that the primary role of the JNK cascade is not the polarization of the DME cells.

JNK-dependent expression of *cbt* in the yolk cell

An interesting observation is that *cbt* expression in the yolk cell nuclei is also dependent on JNK signaling. Our results show that *cbt* expression in that tissue is abolished in embryos mutant for JNK components, although there is no reported evidence that JNK signaling is active in the yolk sac. Then, how could this be achieved? It has been reported that the JNK signaling cascade is active in the amnioserosa and the LE of the epidermis at the beginning of DC. Later on, it is downregulated in the amnioserosa but not in the LE cells and, after closure, it seems to be upregulated again in the amnioserosa to trigger its disintegration and death (Reed et al., 2001; 2004). Recent studies have suggested that the yolk cell is also required for

DC (Narasimha and Brown, 2004; Reed et al., 2004). Indeed, an intimate contact between the amnioserosa and this tissue during DC, which is mediated by integrins, is necessary to prevent anoikis of the amnioserosa. One of these studies has shown that there are cellular extensions that allow contact between both tissues, which led to the proposal that these projections may facilitate a signaling function between them (Reed et al., 2004). Since JNK signaling is active in the amnioserosa during DC, we considered the possibility that this signaling function could explain the JNK-dependent expression of *cbt* in the yolk cell. Our results show that *cbt* expression in that tissue is absent in embryos mutant for *myospheroid*, which encodes the *Drosophila* βPS integrin (MacKrell et al. 1988). In such embryos there are no physical interactions between the amnioserosa and the yolk cell and, in consequence, neither communication nor signaling function between both tissues can exist. It has been proposed that active forms of ecdysone could be transported from the yolk spheres to the amnioserosa (Reed et al., 2004). Although our results do not explain how this signaling could occur or which molecules could be responsible for it, it is tempting to speculate that *cbt* activation in the yolk cell nuclei requires communication between both tissues and implicates the transport of molecules. A more detailed study of the dynamic invaginations seen in the yolk sac membrane, the distribution of Cbt or JNK cascade proteins and their transport between both tissues are necessary to confirm this hypothesis.

A model of Cbt function in the epidermis

Although *cbt* is expressed in the epidermis and the yolk cell nuclei, DC defects observed in *cbt* mutant embryos could be explained considering that Cbt is only required in the epidermis. Indeed, we have shown that the embryonic lethality associated to a *cbt* mutant allele is totally rescued by overexpression of *cbt* with an epidermal driver, but only partially rescued when using a driver specific for the yolk cell. Then, the function of this gene in the yolk cell is still

unknown. Narashima et al. (2004) and Reed et al. (2004) reported that the close apposition of the yolk cell and the amnioserosa is necessary during DC (and germ band retraction). But it remains unclear whether the yolk cell plays an active role during DC or it is only a mechanistic/signaling support to the morphogenesis or survival of the amnioserosa. Further studies will be required to clarify this issue.

As we have shown, the zinc finger protein Cbt is required downstream of JNK signaling to control actomyosin cable assembly at the LE, elongation of the DME cells, but also to maintain *dpp* expression in those cells. Although our results do not address the molecular mechanism, we have proposed several models to explain one of these functions, such as *dpp* activation. One possibility is that Cbt directly activates *dpp* expression by binding to specific enhancers of the gene. In this function Cbt may be acting alone, or it may need putative partners that would cooperate or potentiate its function. Alternatively, we can imagine a different situation where *dpp* activation is not direct but mediated by another gene that would be activated by Cbt. Moreover, Cbt could also activate the expression of other genes necessary for cable assembly or epidermal cell elongation. Several experiments are in progress in our laboratory to identify possible Cbt partners and other genes that could be related to its function. This will help to unravel the exact mechanism of action that allows Cabut to regulate gene expression and to determine the exact role of this gene during DC.

ACKNOWLEDGEMENTS

We are grateful to the Bloomington and Szeged stock centers for fly strains. We thank A. Martínez-Arias, S. Noselli, E. Martín-Blanco J. Karess, J. Reinitz, S. Casas, P. Bryant, D. Yamamoto, R. Bodmer and J.A. Navarro for fly stocks and reagents. We also thank R.D. Artero for critical reading of the manuscript. Confocal and scanning electronic microscopy

was performed at the SCSIE (Universitat de Valencia). S. M.-D. is supported by a fellowship from Consellería de Cultura, Educació i Ciència. This work was supported by grants from the Consellería de Cultura, Educació i Ciència (GV99-120-1-5) and the Ministerio de Educación y Ciencia (BFU2004-00498/BMC) to N. P.

REFERENCES

Brand, A., Perrimon, N., 1993. Targeted gene expression as a means of altering cell fates and generating dominant phenotypes. Development 118, 401-415.

Cheung, H.K., Serano, T.L., Cohen, R.S., 1992. Evidence for a highly selective RNA transport system and its role in establishing the dorsoventral axis of the *Drosophila* egg. Development 114: 653-661.

Digan, M.E., Haynes, S.R., Mozer, B.A., Dawid, I.B., Forquignon, F., Gans, M., 1986. Genetic and molecular analysis of fs(1)h, a maternal effect homeotic gene in *Drosophila*. Dev. Biol. 114: 161-169.

Glise, B., Bourbon, H., Noselli, S., 1995. *hemipterous* encodes a novel *Drosophila* MAP kinase kinase, required for epithelial cell sheet movement. Cell 83, 451-461.

Glise, B., Noselli, S., 1997. Coupling of Jun amino-terminal kinase and Decapentaplegic signaling pathways in *Drosophila* morphogenesis. Genes Dev. 11, 1738-1747.

Harden, N., 2002. Signaling pathways directing the movement and fusion of epithelial sheets: lessons from dorsal closure in *Drosophila*. Differentiation 70, 181-203.

Harden, N., Ricos, M., Yee, K., Sanny, J., Langmann, C., Yu, H., Chia, W., Lim, L., 2002. Drac1 and Crumbs participate in amnioserosa morphogenesis during dorsal closure in *Drosophila*. J. Cell Sci. 115, 2119-2129.

Hou, X.S., Goldstein, E.S., Perrimon, N., 1997. Drosophila Jun relays the Jun amino-terminal kinase signal transduction pathway to the Decapentaplegic signal transduction pathway in regulating epithelial cell sheet movement. Genes Dev. 11, 1728-1737.

Ingham, P.W., Taylor, A.M., Nakano, Y. 1991. Role of the *Drosophila patched* gene in positional signalling. *Nature* 353, 184-187.

Iuchi, S., 2001. Three classes of C2H2 zinc finger proteins. Cell. Mol. Life Sci. 58, 625-635.

Jacinto, A., Martin, P., 2001. Morphogenesis: unravelling the cell biology of hole closure. Curr. Biol. 11, R705-707.

Jacinto, A., Woolner, S., Martin, P., 2002. Dynamic analysis of dorsal closure in *Drosophila*: from genetics to cell biology. Dev. Cell 3, 9-19.

Jordan, P., and Karess, R., 1997. Myosin light chain-activating phosphorylation sites are required for oogenesis in *Drosophila*. J. Cell. Biol. 139, 1805-1819.

Kaltschmidt, J.A., Lawrence, N., Morel, V., Balayo, T., Fernández, B.G., Pelissier, A., Jacinto, A., Martinez Arias, A., 2002. Planar polarity and actin dynamics in the epidermis of *Drosophila*. Nat. Cell Biol. 4, 937-944.

Kiehart, D.P., Galbraith, C.G., Edwards, K.A., Rickoll, W.L., Montague, R.A., 2000. Multiple forces contribute to cell sheet morphogenesis for dorsal closure in *Drosophila*. J. Cell Biol. 149, 471-490.

Kockel, L., Zeitlinger, J., Staszewski, L.M., Mlodzik, M., Bohmann, D., 1997. Jun in *Drosophila* development: redundant and nonredundant functions and regulation by two MAPK signal transduction pathways. Genes Dev. 11, 1748-1758.

Lockwood, W.K., Bodmer, R., 2002. The patterns of *wingless*, *decapentaplegic*, and *tinman* position the *Drosophila* heart. Mech. Dev. 114, 13-26.

MacKrell, A.J., Blumberg, B., Haynes, S.R., Fessler J.H., 1988. The lethal *myospheroid* gene of *Drosophila* encodes a membrane protein homologous to vertebrate integrin beta subunits. Proc. Natl. Acad. Sci. 85, 2633-2637.

Manoukian, A.S, Krause, H.M. 1992. Concentration-dependent activities of the even-skipped protein in Drosophila embryos.*Genes Dev*. 6, 1740-1751.

Martin, P., Wood W., 2002. Epithelial fusions in the embryo. Curr. Opin. Cell Biol. 14, 569-574.

Martin-Blanco, E., Gampel, A., Ring, J., Virdee, K., Kirov, N., Tolkovsky, A.M., Martinez-Arias, A., 1998. *puckered* encodes a phosphatase that mediates a feedback loop regulating JNK activity during dorsal closure in *Drosophila*. Genes Dev. 12, 557-570.

McEwen, D.G., Cox, R.T., Peifer, M., 2000. The canonical Wg and JNK signaling cascades collaborate to promote both dorsal closure and ventral patterning. Development 127, 3607-3617

Miyamoto, H., Nihonmatsu, I., Kondo, S., Ueda, R., Togashi, S., Hirata, K., Ikegami, Y., Yamamoto, D., 1995. *canoe* encodes a novel protein containing a GLGF/DHR motif and functions with Notch and scabrous in common developmental pathways in *Drosophila*. Genes Dev. 9, 612-25.

Morel, V., Martínez-Arias, A., 2004. Armadillo/beta-catenin-dependent Wnt signalling is required for the polarisation of epidermal cells during dorsal closure in *Drosophila*. Development 131, 3273-3283.

Narasimha M., Brown, N.H., 2004. Novel functions for integrins in epithelial morphogenesis. Curr. Biol. 14, 381-385.

Noselli, S., Agnes, F., 1999. Roles of the JNK signaling pathway in *Drosophila* morphogenesis. Curr. Opin. Genet. Dev. 9, 466-472.

Nusslein-Volhard, C., Kluding, H., Jurgens, G. 1985. Genes affecting the segmental subdivision of the Drosophila embryo. *Cold Spring Harbor Symp. Quant. Biol.* 50, 145-154.

Nusslein-Volhard, C., Wieschaus, E., Kluding, H., 1984. Mutations affecting the pattern of the larval cuticle in *Drosophila melanogaster*. Arch. Dev. Biol. 193, 267-282.

Reed, B.H., Wilk, R., Lipshitz, H.D., 2001. Downregulation of Jun kinase signaling in the amnioserosa is essential for dorsal closure of the *Drosophila* embryo. Curr. Biol. 11, 1098-1108.

Reed, B.H., Wilk, R., Schock, F., Lipshitz, H.D., 2004. Integrin-dependent apposition of *Drosophila* extraembryonic membranes promotes morphogenesis and prevents anoikis. Curr. Biol. 14, 372-380.

Ricos, M.G., Harden, N., Sem, K.P., Lim, L., Chia, W., 1999. Dcdc42 acts in TGF-beta signaling during Drosophila morphogenesis: distinct roles for the Drac1/JNK and Dcdc42/TGF-beta cascades in cytoskeletal regulation. J. Cell Sci. 112, 1225-1235.

Riesgo-Escovar, J.R., Hafen, E., 1997. Drosophila Jun kinase regulates expression of *decapentaplegic* via the ETS-domain protein Aop and the AP-1 transcription factor DJun during dorsal closure. Genes Dev. 11, 1717-1727.

Riesgo-Escovar, J.R., Jenni, M., Fritz, A., Hafen, E., 1996. The *Drosophila* Jun-N-terminal kinase is required for cell morphogenesis but not for DJun-dependent cell fate specification in the eye. Genes Dev. 10, 2759-2568.

Ring, J.M., Martínez-Arias, A., 1993. *puckered*, a gene involved in position-specific cell differentiation in the dorsal epidermis of the *Drosophila* larva. Dev. Suppl. 1993, 251-259.

Rørth, P., Szabo, K., Bailey, A., Laverty, T., Rehm, J., Rubin, G. M., Weigmann, K., Milán, M., Benes, V., Ansorge, W., Cohen, S.M., 1998. Systematic gain-of-function genetics in *Drosophila*. Development 125, 1049-1057.

Sanson, B., White, P., Vincent, J.P., 1996. Uncoupling cadherin based adhesion from wingless signalling in *Drosophila*. Nature 383, 627-630.

Sluss, H.K., Han, Z., Barrett, T., Davis, R.J., Ip, Y.T., 1996. A JNK signal transduction pathway that mediates morphogenesis and an immune response in *Drosophila*. Genes Dev. 10, 2745-2758.

Spradling, A.C., Rubin, G.M., 1982. Transposition of cloned P elements into *Drosophila* germ line chromosomes. Science 218, 341-347.

Tabata, T., Schwartz, C., Gustavson, E., Ali, Z., Kornberg, T. 1995. Creating a *Drosophila* wing de novo, the role of engrailed, and the compartment border hypothesis. *Development* 121, 3559-3569.

Takahashi, K., Matsuo, T., Katsube, T., Ueda, R., Yamamoto, D., 1998. Direct binding between two PDZ domain proteins Canoe and ZO-1 and their roles in regulation of the jun N-terminal kinase pathway in *Drosophila* morphogenesis. Mech. Dev. 78, 97-111.

Tautz, D., Pfeifle, C**.,** 1989. A non-radioactive *in situ* hybridization method for the localization of specific RNAs in *Drosophila* embryos reveals translational control of the segmentation gene hunchback. Chromosoma 98, 81-85.

Woods, D.F., Hough, C., Peel, D., Callaini, G., Bryant, P.J., 1996. Dlg protein is required for junction structure, cell polarity, and proliferation control in *Drosophila* epithelia. J. Cell Biol. 134, 1469-1482.

Young, P.E., Richman, A.M., Ketchum, A.S., Kiehart, D.P., 1993. Morphogenesis in *Drosophila* requires nonmuscle myosin heavy chain function. Genes Dev. 7, 29-41.

Zeitlinger, J., Kockel, L., Peverali, F.A., Jackson, D.B., Mlodzik, M., Bohmann, D., 1997. Defective dorsal closure and loss of epidermal *decapentaplegic* expression in *Drosophila fos* mutants. EMBO J. 16, 7393-7401.

FIGURE LEGENDS

Figure 1. Molecular structure of *cabut*. (A) A schematic of the *cabut* gene locus showing the relative position of the *EP(2)2237* element. Coding regions are shown in black, non-coding regions in white, and the intron is depicted as an open triangle. (B) Relative positions of the molecular lesions detected in $cbt^{EP(2)2237E1}$ and $cbt^{EP(2)2237E28}$ alleles and 3´ end of the *cbt* downstream gene *Arc105*. (C) Hypothetical Cbt protein. White boxes represent Zn fingers; squared box indicates a Ser-rich region. (D) Alignment of the three Cbt Zn fingers. Cysteines and histidines are in bold.

Figure 2. *cabut* expression during embryonic development. (A-B, D-E) Whole-mount in situ hybridization with a digoxigenin-labeled *cbt* riboprobe. (A) Wild-type cellular blastoderm embryo. (B) Stage 13 wild type embryo showing *cbt* expression in the yolk nuclei, lateral epidermis and posterior gut (arrow). (C) Magnification of the yolk cell region of a stage 13 $bsg^{B39.1M2}$ embryo doubled stained with β-galactosidase (orange) and *cbt* riboprobe (blue), note that *cbt* RNA and β-gal colocalize in the yolk cell nuclei (arrow). (D and E) Stage 14 $cbt^{EP(2)2237E1}$ and $cbt^{EP(2)223728}$ homozygous mutant embryos, respectively. Note that in while in $cbt^{EP(2)2237E1}$ the *cbt* expression is absent in the yolk and epidermis, it persists in the gut. In $cbt^{EP(2)2237E28}$ the expression is only lost in the yolk cell. A and C are lateral views, B and E are dorsal views and D is a dorso-lateral view. (F) Northern blot analysis on total RNA extracted from w^- (lane 1), $cbt^{EP(2)2237E1}/cbt^{EP(2)2237E1}$ (lane 2), $cbt^{EP(2)2237E28}/cbt^{EP(2)2237E28}$ (lane 3) and *arm*-GAL4/UAS-*cbt* (lane 4) embryos. In $cbt^{EP(2)2237E1}$ embryos *cbt* expression is very reduced, but in $cbt^{EP(2)2237E28}$ is similar to wild type (compare to lane 1). *arm*-GAL4/UAS-*cbt* RNA is a positive control. Expression of *RP49* was used as loading control.

Figure 3. Phenotypic analysis of *cabut* mutant embryos. (A-D) Embryonic cuticle preparations visualized by dark-field optics. (A) Wild-type embryo. (B-C) $cbt^{EP(2)2237E1}$ homozygous mutant embryos. Numbers in B and C represent the percentages of each phenotype seen in the mutant embryos analyzed. (D) $cbt^{EP(2)2237E28}$ homozygous mutant embryo. (E-H) Scanning electron microscopy (SEM) of $cbt^{EP(2)2237E1}$ homozygous mutant embryos. (E) Embryo before dorsal closure (stage 11), (F) during germ-band retraction (stage 12), (G) during dorsal closure (stage 14) and (H) at post-dorsal closure stage (stage 17). Scale bar in E, 150 μm (applicable to F-H). In all cases dorsal is up, except in H that is a dorsal view.

Figure 4. Cell shape changes in the lateral epidermis and the amnioserosa in *cbt* mutant embryos. Confocal fluorescent micrographs, assembled from Z-sections, of the boundary between the amnioserosa (top) and epidermis midway through DC, except E and F that are dorsal views of the amnioserosa. (A, C, E) Wild-type and (B, D, F) $cbt^{EP(2)2237E1}$ homozygous mutant embryos. (A, B) Distribution of FasIII and (C, D) Dlg to reveal the shape and polarity of cells in the dorsal ectoderm. As dorsal closure proceeds, cells of the dorsal epidermis are elongated in the D-V direction and polarized (A, C). Note that in *cbt* mutants dorsal epidermal cells fail to elongate and Dlg or FasIII are occasionally mislocalized to the LE (arrows in B and D). (E, F) Distribution of Cno to outline amnioserosal cells. Note the successful constriction of cells at the ends of the amnioserosa of the *cbt* mutant embryo (arrowheads in F). The arrow points to an amnioserosa-epidermis attachment defect. Scale bar in A, 40μm (applicable to B); scale bar in C and E, 100μm (applicable to D and F, respectively).

Figure 5. Cytoskeleton activity at the leading edge is disturbed in *cbt* mutant embryos. Anti-non muscle myosin II stainings in (A) wild-type and (B) *cbt* mutant embryos to visualize

the contractile cable at the LE. Note the elevated and punctate distribution of myosin in wild-type embryos, which accumulates in large aggregates at the LE. *cbt* mutant embryos show a feeble and irregular accumulation of myosin at the LE, and the protein is depleted in patches (arrows). Scale bar in A, 100μm (applicable to B).

Figure 6. ***cabut* is downstream of JNK signaling**. Distribution of *cbt* RNAs in stage 13 embryos (except D: stage 10 embryo). (A) Wild-type embryo. (B) bsk^2 (C) jun^2, (E-F) mys^1 homozygous embryos. F is a magnification of E. (D) *en*-GAL4/UAS-Hep^{Act} embryo showing ectopic *cbt* expression (arrow points to one example). Note that *cbt* expression is totally absent in *jun* and *bsk* mutant embryos, both in the yolk cell and epidermis. However *cbt* expression in the epidermis persists in mys^1 embryos (E). In the gut, *cbt* expression persists in all mutant embryos. Dorsal is up, except in A that is a dorsal view.

Figure 7. Mutations in *cbt* affect *dpp* but not *puc* expression. (A-F) Whole-mount in situ hybridizations with a digoxigenin-labeled riboprobe for *dpp*. (A) Wild-type embryo at stage 13. (B) $cbt^{EP(2)2237E1}$ homozygous mutant embryo of the same stage. The *dpp* expression at the LE (arrow) depends on JNK signaling, note that this expression is absent from the LE in the *cbt* mutant embryo. (C) Wild-type stage 10 embryo. (E) *arm*-GAL4/UAS-*cbt* embryo. (F) *en*-GAL4/UAS-*cbt* embryo. Note that overexpression of *cbt*, induces ectopical expression of *dpp*. (E-F) *puc* enhancer trap expression. (F) puc^{E69}/+ embryo, (G) $cbt^{EP(2)2237E1}$; puc^{E69}/+ embryo. Note that *puc* expression in the LE cells persists in the *cbt* mutant embryo.

SUPPLEMENTARY DATA

Figure S1. PCR analysis of the *cbt* upstream region. (A) Scheme of the *cbt* genomic region showing the position of PCR fragments (1-5) amplified using overlapping primers (arrows). (B) Gel electrophoresis of the PCR fragments. Each PCR analysis was performed using genomic DNA extracted from *EP(2)2237* flies (fragments 1a, 2a, 3a, 4a and 5a) and from $cbt^{EP(2)2237E1}$ mutant embryos(fragments 1b, 2b, 3b, 4b and 5b); VI indicates the molecular weight marker (Roche), – is the PCR negative control. All PCR reactions were performed simultaneously and with the same amounts of genomic DNA: Note that the fragment 5 is amplified in *EP(2)2237* flies but is weakly amplified in $cbt^{EP(2)2237E1}$ mutant embryos. Since the embryos used for DNA extraction were not dechorionized, marginal amplification is detected in the mutants.

Figure1

Click here to download high resolution image

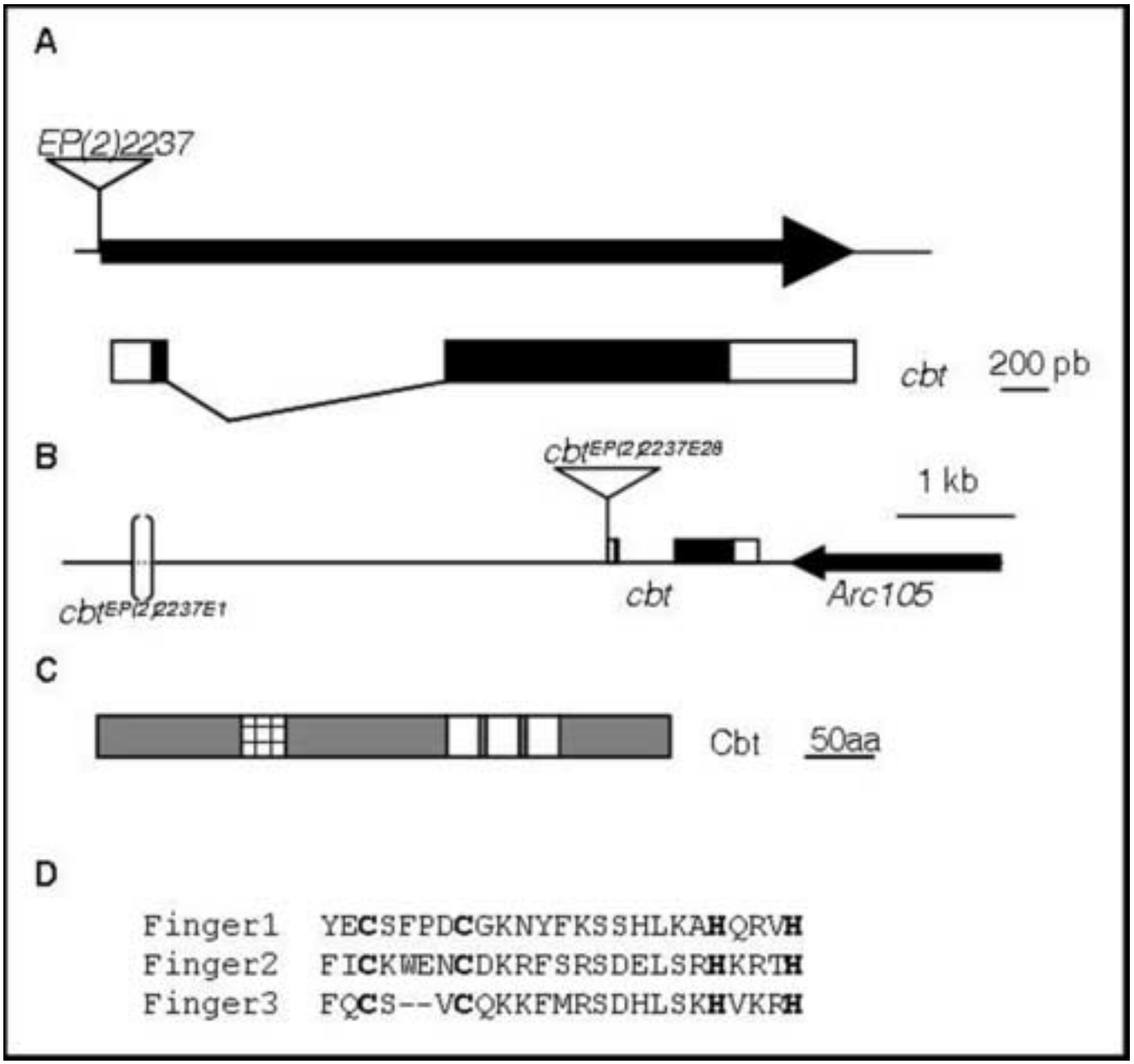

Figure2

Click here to download high resolution image

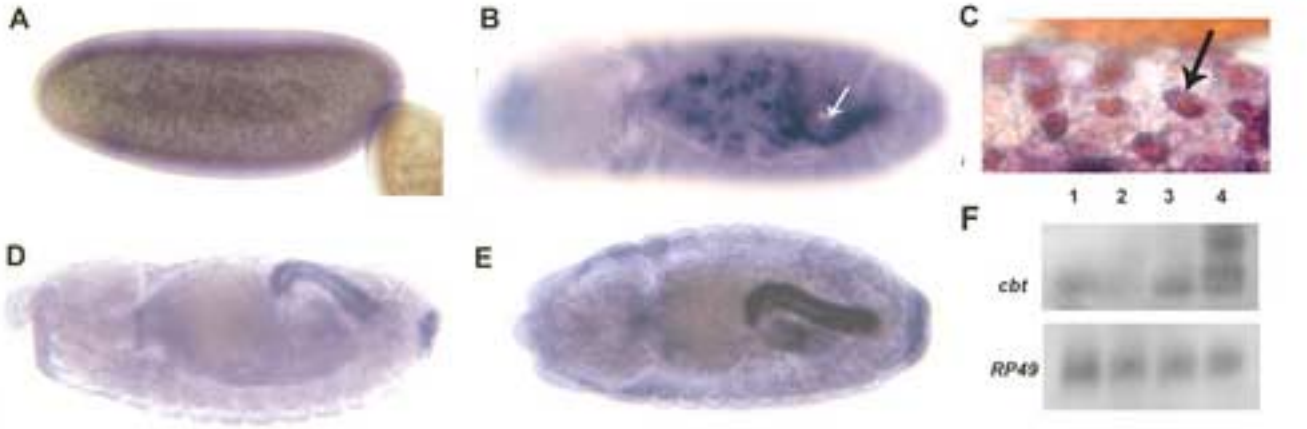

Figure3
Click here to download high resolution image

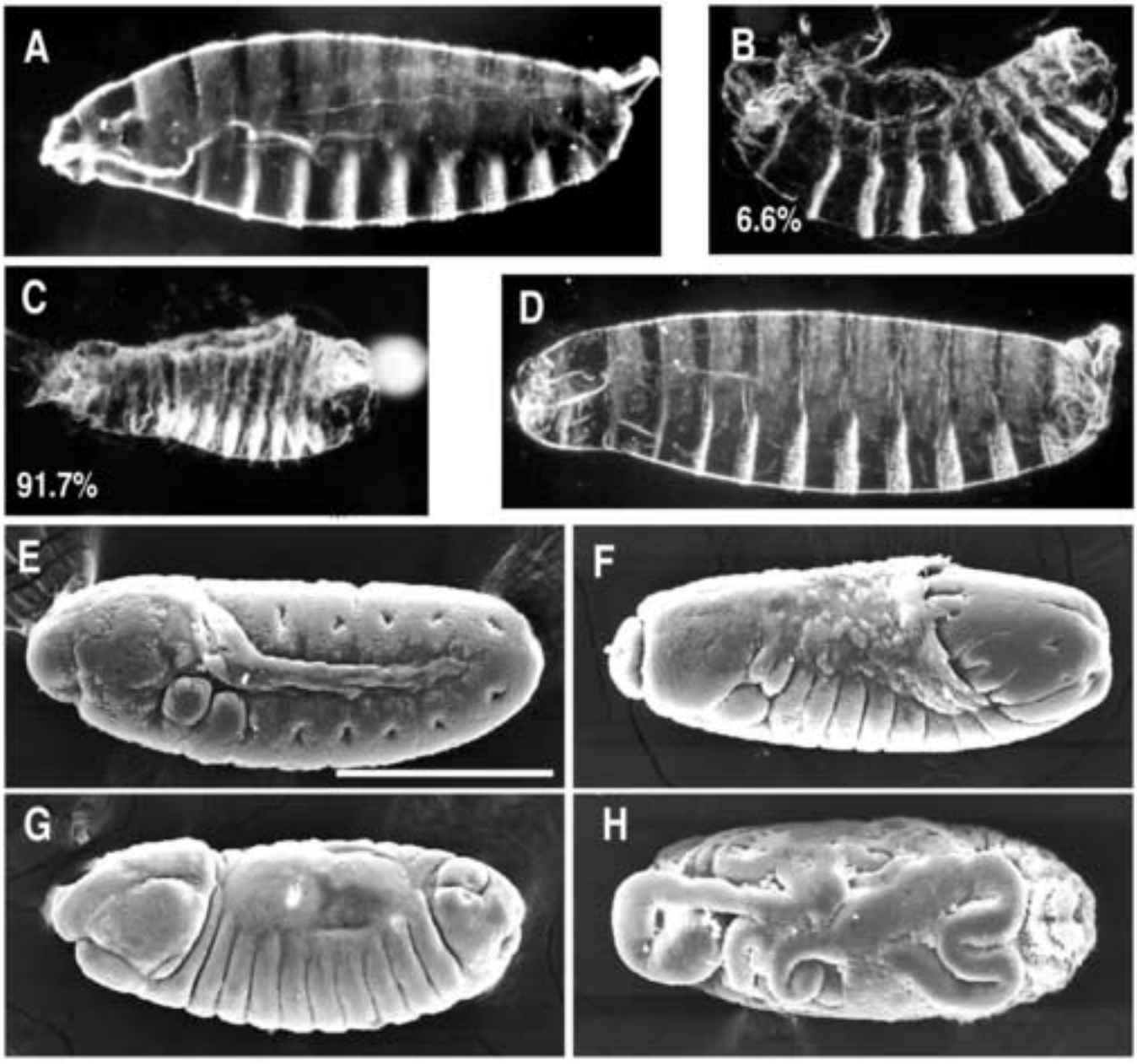

Figure4

Click here to download high resolution image

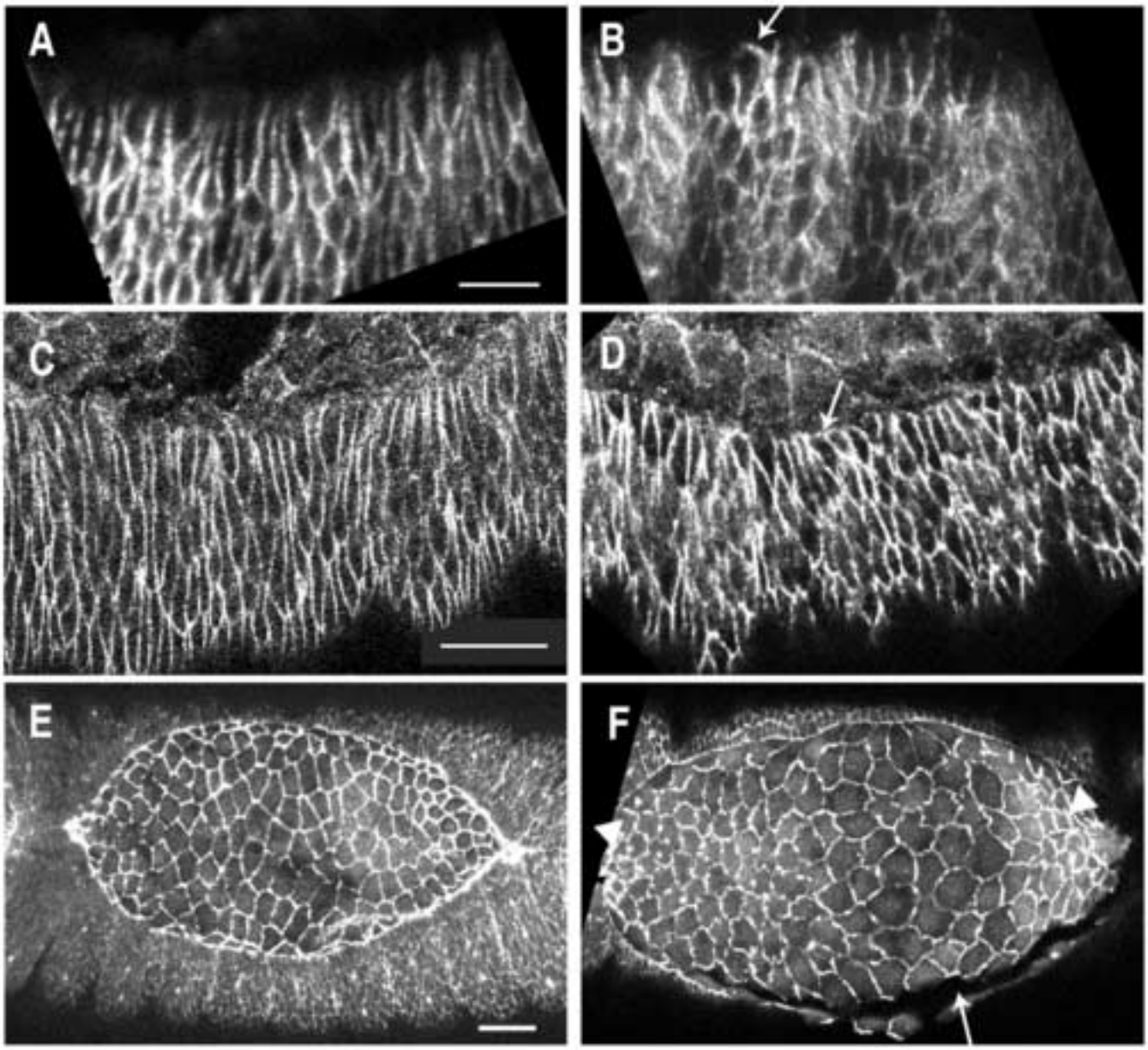

Figure5

Click here to download high resolution image

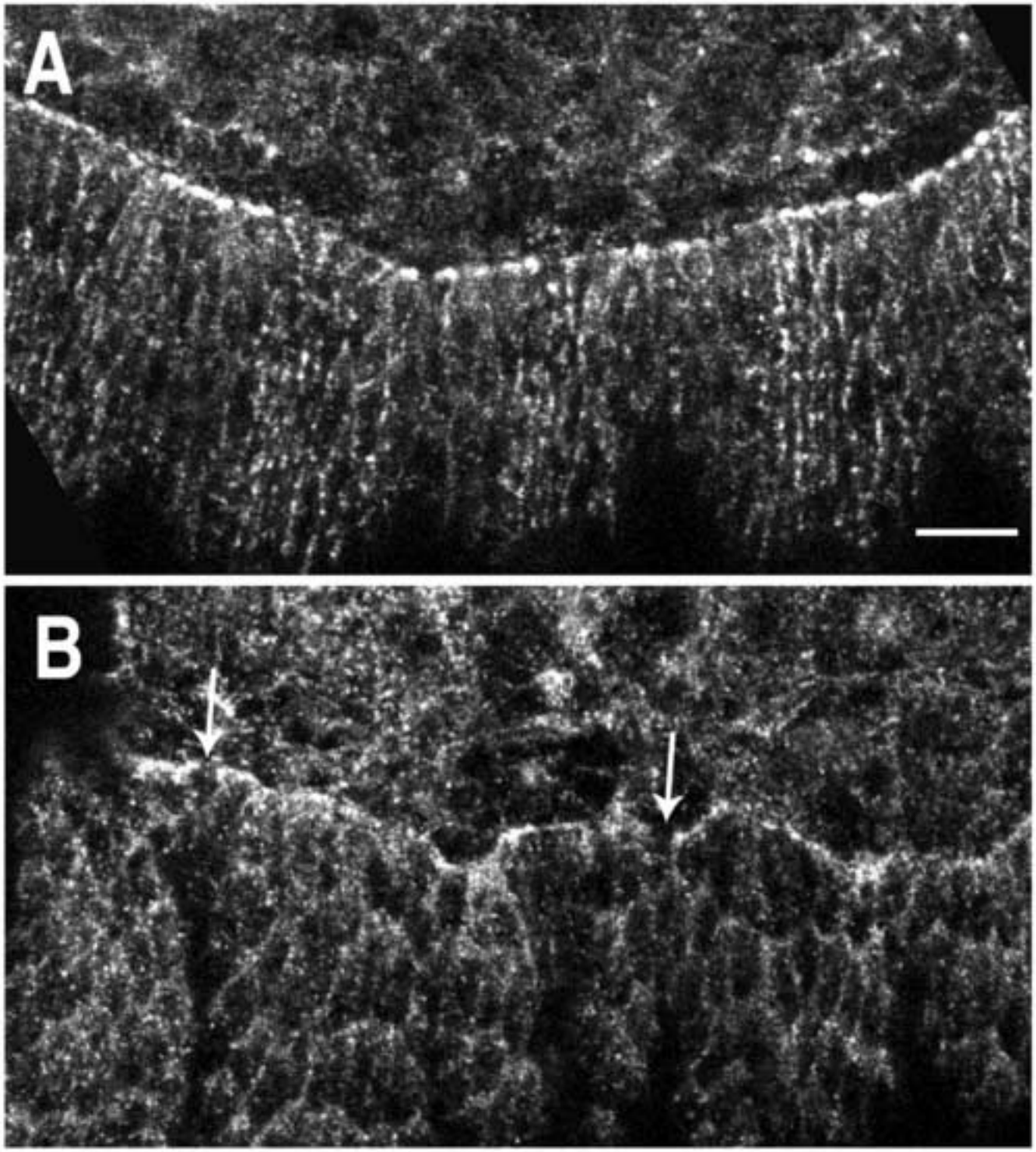

Figure6

Click here to download high resolution image

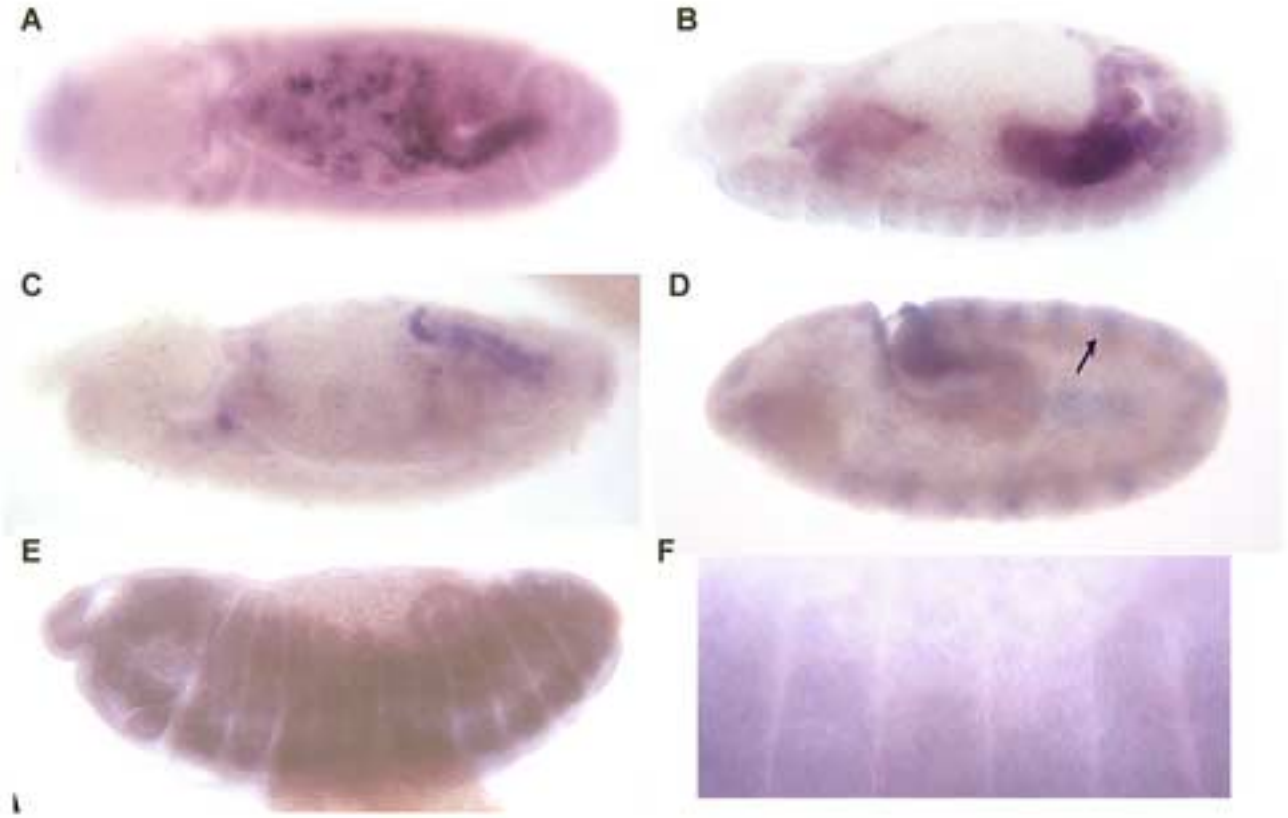

Figure7

Click here to download high resolution image

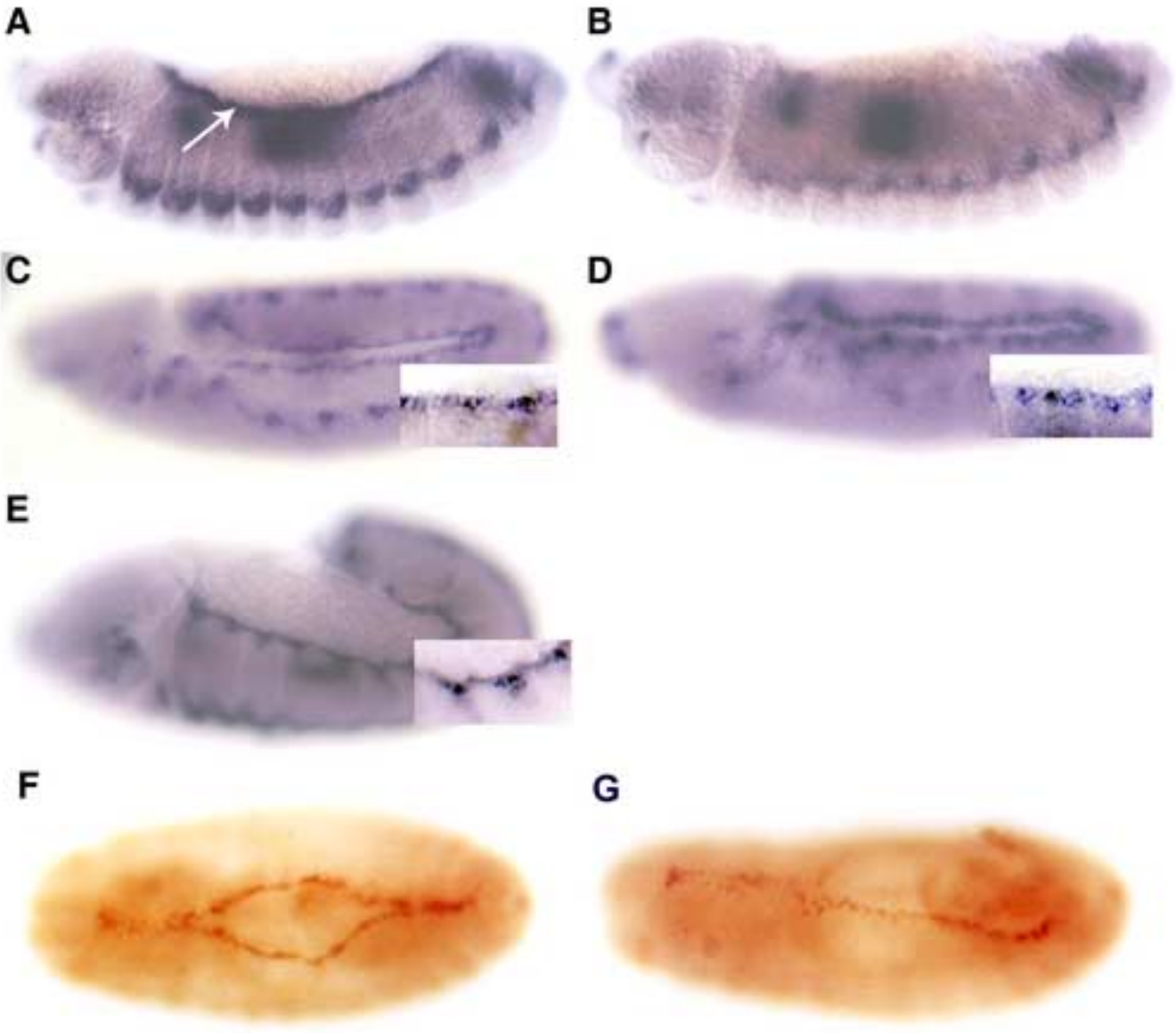

Table1

Table 1. Lethality rescue assays

Genotype	Lethal embryos/Total	Lethality rescue
cbt$^{EP(2)2237E1}$/*cbt*$^{EP(2)2237E1}$;*da*-GAL4/UAS-*cbt*	447/2045	50.2% [a]
cbt$^{EP(2)2237E1}$/*cbt*$^{EP(2)2237E1}$;*69B*-GAL4/UAS-*cbt*	329/1858	100% [a]
cbt$^{EP(2)2237E1}$/*cbt*$^{EP(2)2237E1}$;*P0180*-GAL4/UAS-*cbt*	398/1873	60% [a]
UAS-*dpp*;*cbt*$^{EP(2)2237E1}$/*cbt*$^{EP(2)2237E1}$;*69B*-GAL4/+	575/2757	66.2% [a]

[a] Embryonic rescue is expressed as a percentage of the expected maximum of 6.25%

Table2

Table 2. Genetic interaction assay between *hep* and *cbt*

Genotype	Lethal embryos/Total	Embryonic lethality
UAS-Hep^{Act}/+;*69B*-GAL4/+	1203/1203	100%
UAS-Hep^{Act}/$cbt^{EP(2)2237E1}$;*69B*-GAL4/+	440/1290	36.4% [a]

[a] Embryonic lethality is expressed as a percentage of the expected maximum of 25%

Supplementary Material

Click here to download high resolution image